

Title	Surface properties of a single perfluoroalkyl group on water surfaces studied by surface potential measurements
Author(s)	Shimoaka, Takafumi; Tanaka, Yuki; Shioya, Nobutaka; Morita, Kohei; Sonoyama, Masashi; Amii, Hideki; Takagi, Toshiyuki; Kanamori, Toshiyuki; Hasegawa, Takeshi
Citation	Journal of Colloid and Interface Science (2016), 483: 353-359
Issue Date	2016-12-01
URL	<a href="http://hdl.handle.net/2433/216978">http://hdl.handle.net/2433/216978</a>
Right	© 2016. This manuscript version is made available under the CC-BY-NC-ND 4.0 license <a href="http://creativecommons.org/licenses/by-nc-nd/4.0/">http://creativecommons.org/licenses/by-nc-nd/4.0/</a> ; The full-text file will be made open to the public on 1 December 2018 in accordance with publisher's 'Terms and Conditions for Self-Archiving'.; This is not the published version. Please cite only the published version. この論文は出版社版ではありません。引用の際には出版社版をご確認ご利用ください。
Type	Journal Article
Textversion	author

1

# 2 Surface Properties of a Single Perfluoroalkyl Group

## 3 on Water Surfaces Studied by Surface Potential

## 4 Measurements

5 *Takafumi Shimoaka<sup>a</sup>, Yuki Tanaka<sup>a</sup>, Nobutaka Shioya<sup>a</sup>, Kohei Morita<sup>b</sup>,*

6 *Masashi Sonoyama<sup>b</sup>, Hideki Amii<sup>b</sup>, Toshiyuki Takagi<sup>c</sup>, Toshiyuki Kanamori<sup>c</sup>,*

7 *Takeshi Hasegawa<sup>\*a</sup>*

8 <sup>a</sup>Laboratory of Solution and Interface Chemistry, Division of Environmental Chemistry,  
9 Institute for Chemical Research, Kyoto University, Gokasho, Uji, Kyoto 611-0011,

10 Japan

11 <sup>b</sup>Division of Molecular Science, Faculty of Science and Technology, Gunma University,  
12 Kiryu, Gunma 376-8515, Japan

13 <sup>c</sup>National Institute of Advanced Industrial Science and Technology (AIST), AIST  
14 Tsukuba Central 5, 1-1-1 Higashi, Tsukuba, Ibaraki 305-8565, Japan

15 E-mail address: [TS] [shimoaka@scl.kyoto-u.ac.jp](mailto:shimoaka@scl.kyoto-u.ac.jp) [YT] [yuki@env.kuicr.kyoto-u.ac.jp](mailto:yuki@env.kuicr.kyoto-u.ac.jp)

16 [NS] [nobutaka@env.kuicr.kyoto-u.ac.jp](mailto:nobutaka@env.kuicr.kyoto-u.ac.jp) [KM] [t09301167@gunma-u.ac.jp](mailto:t09301167@gunma-u.ac.jp)

17 [MS] [sonoyama@gunma-u.ac.jp](mailto:sonoyama@gunma-u.ac.jp) [HA] [amii@gunma-u.ac.jp](mailto:amii@gunma-u.ac.jp) [TT] [t.takagi@aist.go.jp](mailto:t.takagi@aist.go.jp)

18 [TK] [t.kanamori@aist.go.jp](mailto:t.kanamori@aist.go.jp) [TH] [htakeshi@scl.kyoto-u.ac.jp](mailto:htakeshi@scl.kyoto-u.ac.jp)

19

20

1    **\*Corresponding Author:** Prof. Takeshi Hasegawa

2           Postal address: Laboratory of Solution and Interface Chemistry, Division of  
3                           Environmental Chemistry, Institute for Chemical Research, Kyoto  
4                           University, Gokasho, Uji, Kyoto 611-0011, Japan

5           Phone:        +81 774 38 3070

6           FAX:         +81 774 38 3074

7           E-mail:        [htakeshi@scl.kyoto-u.ac.jp](mailto:htakeshi@scl.kyoto-u.ac.jp)

8

9

10   **Highlights:**

- 11    ● Dehydration about the head group is a key to understand surface potential changes.
- 12    ● A single perfluoroalkyl group is stabilized on a water surface.
- 13    ● A long perfluoroalkyl chain makes a stiff molecular domain on the water surface.

14

1 **Abstract:** A discriminative study of a single perfluoroalkyl (Rf) group from a bulk  
2 material is recently recognized to be necessary toward the total understanding of Rf  
3 compounds based on a primary chemical structure. The single molecule and the bulk  
4 matter have an interrelationship via an intrinsic two-dimensional (2D) aggregation  
5 property of an Rf group, which is theorized by the stratified dipole-arrays (SDA) theory.  
6 Since an Rf group has dipole moments along many C–F bonds, a single Rf group would  
7 possess a hydrophilic-like character on the surface. To reveal the hydration character of  
8 a single Rf group, in the present study, surface potential ( $\Delta V$ ) measurements are  
9 performed for Langmuir monolayers of Rf-containing compounds. From a comparative  
10 study with a monolayer of a normal hydrocarbon compound, the hydration/dehydration  
11 dynamics of a lying Rf group on water has first been monitored by  $\Delta V$  measurements,  
12 through which a single Rf group has been revealed to have a unique “dipole-interactive”  
13 character, which enables the Rf group interacted with the water ‘surface.’ In addition,  
14 the SDA theory proves to be useful to predict the 2D aggregation property across the  
15 phase transition temperature of 19 °C by use of the  $\Delta V$  measurements.

16 **Keywords:** Langmuir monolayer; surface potential; single perfluoroalkyl chain; water  
17 surface  
18

1 **Introduction:** Perfluoroalkyl (Rf) compounds exhibit unique “bulk characters”  
2 represented by the high water- and oil-repelling property, low dielectric permittivity, and  
3 low solubility in a solvent, which have long been used extensively for many practical  
4 chemical products.<sup>1</sup> When a local structure of the Rf group is taken into account,  
5 however, uniformed understanding of the bulk properties is difficult. For example, the  
6 C–F bond has a large dipole moment due to the largest electronegative character of  
7 fluorine,<sup>2,3</sup> which should attract water molecule via the dipole-dipole interaction. This  
8 fact seems inconsistent with the hydrophobic surface property on Rf compounds.  
9 Recently, a novel chemical theory, i.e., the stratified dipole-arrays (SDA) theory, has  
10 been proposed for fully understanding the material characters, which discriminates a  
11 ‘single molecular character’ from the ‘bulk one.’<sup>4</sup>

12 This theory is based on the dipole-dipole interaction<sup>5</sup> of the Rf groups having a  
13 helical structure.<sup>1,6,7</sup> In Rf compounds, the Rf chains are aggregated tightly by  
14 two-dimensional dipole-dipole interaction arrays, in which all the dipoles corresponding  
15 to CF<sub>2</sub> groups are linearly aligned in the head-to-tail manner. The tight aggregation  
16 readily explains most of the bulk characters comprehensively<sup>4</sup>. Fortunately, this theory  
17 readily covers the conventional polarizability-based theory<sup>8</sup> to account for the low  
18 permittivity. Since the intrinsic difference between an Rf group and a normal

1 hydrocarbon is attributed<sup>9</sup> to the difference between the dipole-dipole interaction and  
2 the dispersion force,<sup>5</sup> respectively, the SDA theory built on the dipole-dipole interaction  
3 has become very important. In particular, the SDA theory is the only theory accounting  
4 for the discontinuity of the melting point<sup>4</sup> at the length of  $-C_8F_{17}$  as well as the  
5 fluorophilic effect<sup>10</sup> and the low electric permittivity, which are not found in a normal  
6 hydrocarbon material.

7         Some of the ‘single molecular characters’ predicted by the SDA theory have  
8 experimentally been confirmed via the adsorption of ‘molecular water’ on a stretched  
9 polytetrafluoroethylene (PTFE; known as Teflon<sup>®</sup>) tape by using <sup>1</sup>H NMR<sup>11</sup>. A PTFE  
10 tape is made of bundled fibrils of polymeric Rf chains with the SDA packing. If the  
11 tape is mechanically stretched, then the SDA packed fibrils are partly disaggregated,  
12 and a single-molecule character of an Rf chain faces to the air. Since a single Rf group  
13 possesses strong dipole moments on the surface due to the C–F bonds, molecular water  
14 having a large dipole should be adsorbed on the surface via the dipole-dipole  
15 interaction. The <sup>1</sup>H NMR study reveals that the adsorption is due to the dipole-dipole  
16 interaction in fact by the chemical shift and  $T_1$  analyses.

17         Judging from an electrodynamics theory,<sup>9</sup> both stretched and un-stretched PTFE  
18 tapes should exhibit ‘hydrophobicity’ to a water ‘droplet’ (not molecular water), since

1 the polarization density (summation of dipole moment in a macroscopic scale)  
2 becomes nearly zero for both cases. In fact, a large contact angle is commonly obtained  
3 for both cases<sup>11</sup>.

4 This implies that the attraction character of a single Rf group to a molecular  
5 water should be discriminated from the general concept of hydrophilicity, and the  
6 character is thus called “dipole-interactive property” throughout this paper. In the  
7 present study, the physical character of a single Rf group is investigated at the air/water  
8 interface. Water surface is known to have some hydrogen-bond free (dangling) OH  
9 groups,<sup>12</sup> which should be a good field to study a single Rf group on the concept of the  
10 dipole-interactive property.

11 A study using a spread monolayer on water (Langmuir (L) film) and the  
12 Langmuir-Blodgett (LB) film is a key approach to investigate properties of a  
13 two-dimensional (2D) molecular aggregate.<sup>13</sup> In fact, the SDA theory has already  
14 proved to be powerful to predict the material property of a compound by the surface  
15 pressure ( $\pi$ )–surface area ( $A$ ) isotherm measurement of the L film and a spectroscopic  
16 study of the LB film.<sup>4</sup> For example, according to the theory, a compound containing a  
17 short Rf-group ( $\text{CF}_3(\text{CF}_2)_6-$  or shorter) should exhibit the dipole interactive or  
18 hydrophilic character, especially when the compound is spread on water: the spread

1 molecules are not aggregated, and they are lying on the water surface.<sup>4</sup> In fact, the  
2 monolayer stays on pure water stably, and the lift-off surface area is apparently larger  
3 than that of a similar compound having no Rf group.<sup>13</sup> This implies that the short-Rf  
4 containing compounds are not dissolving into water, but it is strongly interacted with the  
5 water ‘surface.’ In this manner, a single Rf group should have a unique attracting  
6 character with the water surface, which is not found for a normal hydrocarbon.

7         To reveal the unique property of an Rf group on a water surface, in the present  
8 study, the surface potential ( $\Delta V$ )–surface area ( $A$ ) isotherms are measured for some  
9 Rf-containing myristic acid (MA) derivatives having an Rf group with a different length,  
10 which are cooperatively discussed with the  $\pi$ – $A$  isotherms. As a result, a notable  
11 molecular aggregation property depending on both Rf length and temperature is  
12 revealed. Thus far,  $\Delta V$ – $A$  isotherms have been discussed in terms of molecular  
13 orientation change after Gains’s textbook.<sup>15</sup> In the present study, however, additional  
14 two factors are found necessary: the molecular density change and the dehydration  
15 about the head group on the monolayer compression. The dehydration is particularly  
16 useful to discuss the dipole-interactive property on the water surface, since the  
17 dipole-shielding by the hydration water is broken by the monolayer compression.

18         In addition, the  $\Delta V$ – $A$  isotherms reveal that bulk properties on the phase



1 transition can also be predicted by the SDA theory. The measurements have all been  
2 performed thus far at 15 °C (Phase II) below the transition temperature at 19 °C.<sup>16</sup> If the  
3 Rf compounds obey the phase diagram,<sup>16</sup> the SDA theory should readily predict the  
4 bulk properties at another temperature above 19 °C (i.e., Phase IV<sup>16</sup>). In the present  
5 study, the same analysis is also performed at 25 °C in Phase IV, and the SDA theory has  
6 proved to be powerful for explaining the phase transition. This is the first report to our  
7 knowledge that the bulk characters of Rf-containing compounds are predicted based on  
8 the primary chemical structure.

9

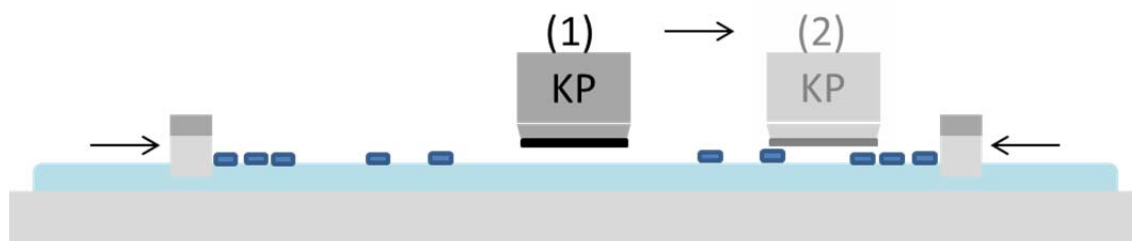
## 10 **Materials and methods:**

11 **Sample preparation:** Octadecanoic acid (stearic acid, SA,  $\geq 98.5\%$ ), tetradecanoic  
12 acid (myristic acid, MA,  $\geq 99\%$ ) and chloroform (ACS Spectra Grade,  $\geq 99.8\%$ ) were  
13 purchased from Sigma-Aldrich (St. Louis, MO, USA), and they were used as is without  
14 further purification. 11,11,12,12,13,13,14,14,14-Nonafluorotetradecanoic acid (MA–  
15 Rf3), 9,9,10,10,11,11,12,12,13,13,14,14,14-tridecafluorotetradecanoic acid (MA–Rf5),  
16 7,7,8,8,9,9,10,10,11,11,12,12,13,13,14,14,14-heptadecafluorotetradecanoic acid (MA–  
17 Rf7) and 5,5,6,6,7,7,8,8,9,9,10,10,11,11,12,12,13,13,14,14,14-henicosafuorotetra-  
18 decanoic acid (MA–Rf9) were synthesized as mentioned in our previous work.<sup>4</sup> Each

1 amphiphilic compound was dissolved in chloroform with a concentration of 0.2–1.0 mg  
2 mL<sup>-1</sup> for preparation of a Langmuir monolayer on water.

3  **$\pi$ -A and  $\Delta V$ -A measurements:** The  $\pi$ -A and  $\Delta V$ -A isotherms were simultaneously  
4 measured by using a Biolin Scientific (Espoo, Finland) KSV-NIMA Minitrough  
5 Langmuir-Blodgett system equipped with a KSV-NIMA SPOT Kelvin probe. The  $\pi$  was  
6 measured by the Wilhelmy method using a paper plate with a width of 1 cm, and  $\Delta V$   
7 was measured by using the Kelvin probe with a counter electrode made of stainless  
8 steel.<sup>17</sup> The Kelvin probe (KP) was located at the position (1) in Chart 1. Each isotherm  
9 was measured three times to check the reproducibility. The water subphase and room  
10 temperature were both maintained at 15 °C or 25 °C to keep the phase II (<19 °C) or IV  
11 (>19 °C), respectively. Pure water subphase was obtained by a Millipore (Molsheim,  
12 France) Elix UV-3 pure-water generator and a Yamato (Tokyo, Japan) Autopure  
13 WT100U water purifier (a compatible model with Milli-Q). The water exhibited an  
14 electric resistivity of 18.2 M $\Omega$  cm or higher. The surface tension was 72.5 mN m<sup>-1</sup> at  
15 25 °C, which was measured by using a Kyowa Interface Science Co., Ltd. (Saitama,  
16 Japan) DropMaster, DM-501Hy, contact angle meter. The Langmuir monolayer was  
17 prepared by spreading the chloroform solution of the amphiphilic compounds on pure  
18 water subphase with a size of 75×324 mm<sup>2</sup>. Each isotherm was measured with a

1 compression rate of  $1.688 \times 10^3 \text{ mm}^2 \text{ min}^{-1}$ .



4 Chart 1 The relative position of the Kelvin probe to the trough. The dark blue  
5 objects are island domains of a Langmuir film. The surface potential ( $\Delta V$ ) of  
6 the film is measured at the position (1) except for the purple dash line in  
7 Figure 3a, which is measured at the position (2).

8

9 The isotherms were measured on pure water (ca. pH 5.8) to make the potential  
10 measurements free from a chemical interference due to a pH modifier. For only MA, the  
11 isotherms were measured at pH 2.0; otherwise the shorter compound than SA is  
12 dissolved into the subphase.<sup>15</sup> The isotherms of a MA monolayer were measured on a  
13 subphase of pH 2.0 involving hydrochloride to prevent the dissolution of the monolayer  
14 into the subphase.<sup>12</sup>

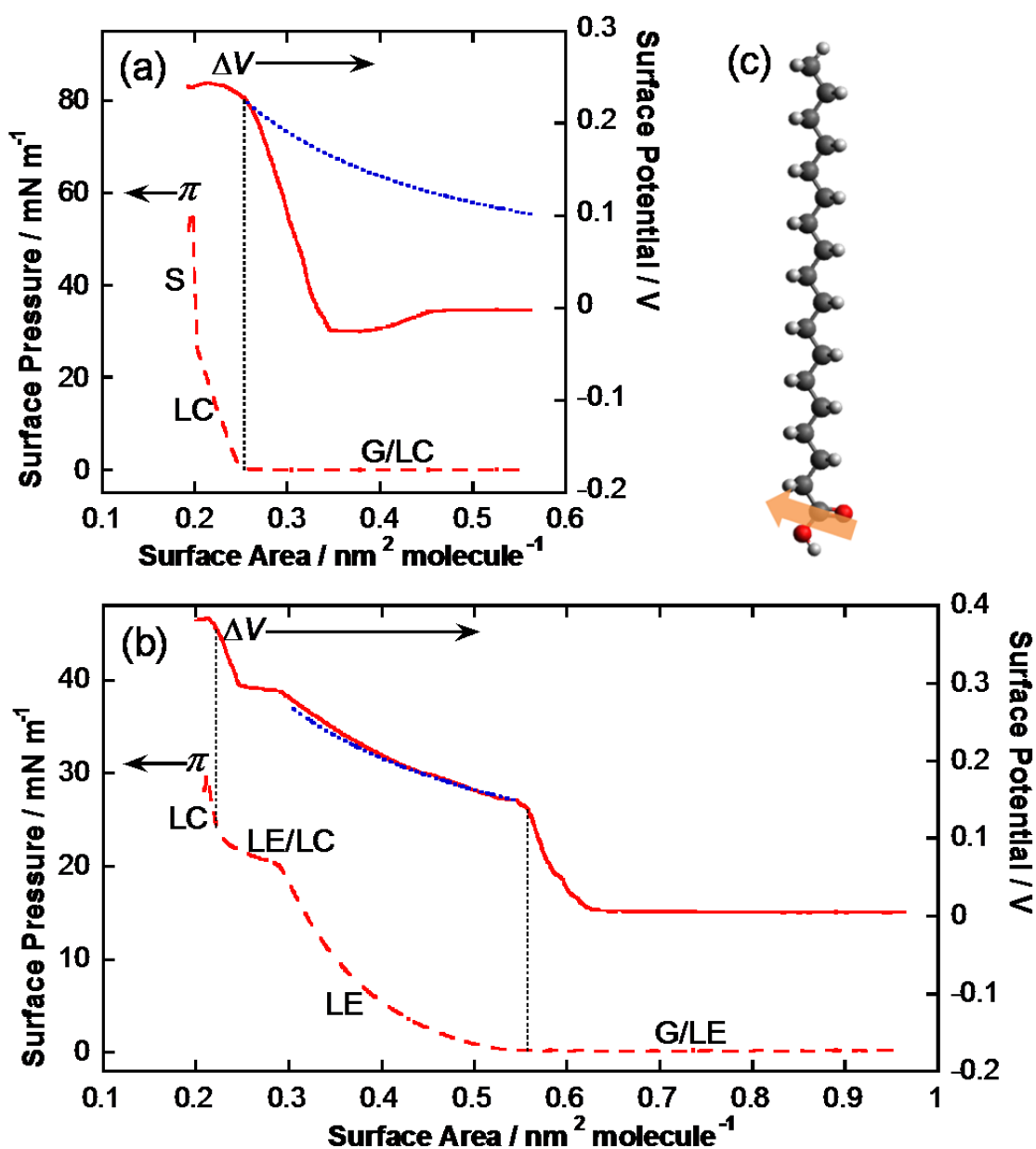
15

16 **Results and Discussion:** The variation of  $\Delta V$  during the monolayer compression ( $\Delta V$ -  
17  $A$ ) is discussed with related to the corresponding  $\pi$ - $A$  isotherm. A  $\Delta V$ - $A$  isotherm of a  
18 Langmuir monolayer (L film) is often discussed in terms of only the molecular  
19 orientation change of a chemical group having a large dipole moment.<sup>18</sup> In the following

1 sections, we show that a  $\Delta V$ - $A$  isotherm reflects two other factors, molecular density  
2 and dehydration about a polar head group, as well as the orientation change, which has  
3 an apparent correlation with the  $\pi$ - $A$  isotherm. Before discussing the Rf-containing  
4 compounds, L films of commonly known stearic acid (SA) and MA are thus used to  
5 show the newly found key factors.

#### 6 **$\Delta V$ - $A$ isotherm of a Normal Carboxylic Acid:**

7 Figure 1a presents  $\pi$ - $A$  and  $\Delta V$ - $A$  isotherms of an L film of SA measured at  
8 25 °C. The  $\pi$ - $A$  isotherm has a typical shape consisting of the well-known three regions:  
9 the gaseous and liquid condensed (G/LC), LC (or “tilted condensed”) and solid (S, or  
10 “un-tilted condensed”) phase regions.<sup>19,20</sup> The electric dipole moment of SA is localized  
11 near the C=O group, but the moment (1.50 D)<sup>21</sup> is tilted to have the upward component  
12 (Figure 1c). Thus, the dipole moment can readily be monitored by the Kelvin probe  
13 even when the molecule has a perpendicular stance to the water surface.<sup>15</sup> In fact,  $\Delta V$   
14 positively appears in the S phase. Note that the  $\Delta V$ - $A$  isotherm seems not synchronous to  
15 the  $\pi$ - $A$  curve (Figure 1a). In particular,  $\Delta V$  begins to increase at ca.  $A = 0.35 \text{ nm}^2$   
16  $\text{molecule}^{-1}$ , which is apparently larger than the lift-off of  $\pi$  (ca.  $0.25 \text{ nm}^2 \text{ molecule}^{-1}$ ) in  
17 the G/LC region.



1  
 2 Figure 1. The  $\pi$ -A (dashed red line) and  $\Delta V$ -A (solid red line) isotherms of a  
 3 Langmuir monolayer of (a) stearic acid (SA) and (b) myristic acid (MA)  
 4 measured at 25 °C. The blue dotted line in the panel (a) and (b) is a  
 5 calculated “density curve” (see the text for detail). (c) A molecular  
 6 schematic of stearic acid. The orange arrow represents the molecular dipole  
 7 moment calculated by a quantum chemical calculation.

8

9

1           In this region, the monolayer compression corresponds to the collection of the  
2 island domains as confirmed by the Brewster angle microscopic study,<sup>22</sup> which accounts  
3 for no increase of the surface pressure ( $\pi \approx 0$ ). The domain is actually an aggregate of  
4 loosely packed SA molecules, but the aggregation property is apparently larger than MA  
5 because of the difference of the chain length.<sup>23</sup>

6           Once  $\Delta V$  begins to increase, the slope should be influenced by changes of the  
7 molecular density and the orientation. Before attaining the LC region (i.e., in the G/LC  
8 region), fortunately, the orientation change can be ignored. To consider the density  
9 change, a theoretical “density curve” is calculated by Eq. 1.

$$10 \quad \Delta V_{\text{density}} = \Delta V_0 A_0 / A. \quad (1)$$

11  $A$  is the surface area and  $A_0$  is the end area of the G/LC region exhibiting  $V_0$ . The point,  
12  $(A_0, \Delta V_0)$  is read from the isotherm to be (0.254, 0.225), and the calculated density  
13 curve is presented by the blue dotted curve in Figure 1a. As a result, the density curve  
14 cannot quantitatively explain the  $\Delta V$ - $A$  curve at all, which straightforwardly implies  
15 that the third factor should be considered. To explain the sudden appearance of  $\Delta V$  at  
16 about  $0.35 \text{ nm}^2 \text{ molecule}^{-1}$ , not only the hydrocarbon chain of SA, but also the head  
17 group should also be taken into account.

18           When the carboxylic group is fully hydrated, the dipole moment is effectively

1 shielded by the dipoles of surrounding water molecules. This explains that  $\Delta V$  exhibits  
2 nearly zero at a surface area larger than ca.  $0.35 \text{ nm}^2 \text{ molecule}^{-1}$ . On a further  
3 compression,  $\Delta V$  runs up to  $0.23 \text{ V}$  before  $\pi$  increases. This sudden appearance of  $\Delta V$  is  
4 understandable by considering the removal of the hydration water by the monolayer  
5 compression. In other words, the dehydration about the carboxylic group is induced by  
6 the monolayer compression, after which the molecules are aggregated resulting in the  
7 increase of  $\pi$ . Therefore, the lift-off of  $\pi$  is always found at the surface area where the  
8 increase of  $\Delta V$  finishes. In the S region, no potential change is monitored, which is  
9 reasonable when considering that almost no change in the density, orientation and  
10 dehydration is expected in the very little change of the surface area.

11 In this manner, by considering the dehydration process, the variations of  $\pi$  and  
12  $\Delta V$  on the compression are comprehensively explained. The relative position of the  
13 increase of  $\pi$  and  $\Delta V$  is thus found very useful to discuss the dehydration; whereas the  
14 absolute value of  $\Delta V$  is not so important.

15 On this fundamental mechanism, the isotherms of an L film of MA are next  
16 discussed. When a monolayer of MA is compressed on pure water (pH 5.8), the  $\pi$ - $A$   
17 isotherm shifts to a smaller area due to the dissolution of the molecules into the  
18 subphase because the carboxylic group of MA are partially ionized<sup>24</sup>. To prevent the

1 matter, the isotherms of only MA were measured at pH 2.0. A  $\pi$ - $A$  isotherm of the MA  
2 at pH 2.0 is a little bit shifted to a larger area than that on pure water. Fortunately,  
3 however,  $\Delta V$ - $A$  curve also exhibits the same shift. Therefore, the discussion of the  
4 relative position between the  $\pi$ - $A$  and  $\Delta V$ - $A$  isotherms is impervious to pH.

5 The isotherms are presented in Figure 1b. The  $\pi$ - $A$  isotherm of the MA  
6 monolayer involves the LE and LE/LC phases in addition to the SA isotherm. This is  
7 because the molecular aggregation property of MA, having shorter alkyl chain, is  
8 weaker than that of SA.<sup>19</sup>

9 In the case of MA,  $\Delta V$  keeps nearly zero until ca.  $0.63 \text{ nm}^2 \text{ molecule}^{-1}$  and  
10 suddenly increases up to 0.15 V before  $\pi$  increases (Figure 1c). This can be explained  
11 by the dehydration model as found for SA. In the LE region,  $\Delta V$  increases almost along  
12 the density curve (blue dotted curve in Figure 1c, calculated by Eq. 1 with  $(A_0, \Delta V_0) =$   
13  $(0.544, 0.150)$ ), which suggests that the potential change can simply be attributed to the  
14 increase of molecular density only.

15 The LE/LC region is known to correspond to the molecular orientation change  
16 during the film compression.<sup>19</sup>  $\Delta V$  in the LE/LC region keeps almost a constant value.  
17 This means that a decrease of  $\Delta V$  due to the orientation change cancels the density  
18 contribution. The decrease is attributed to the orientation change of MA having the



1 carboxylic group.

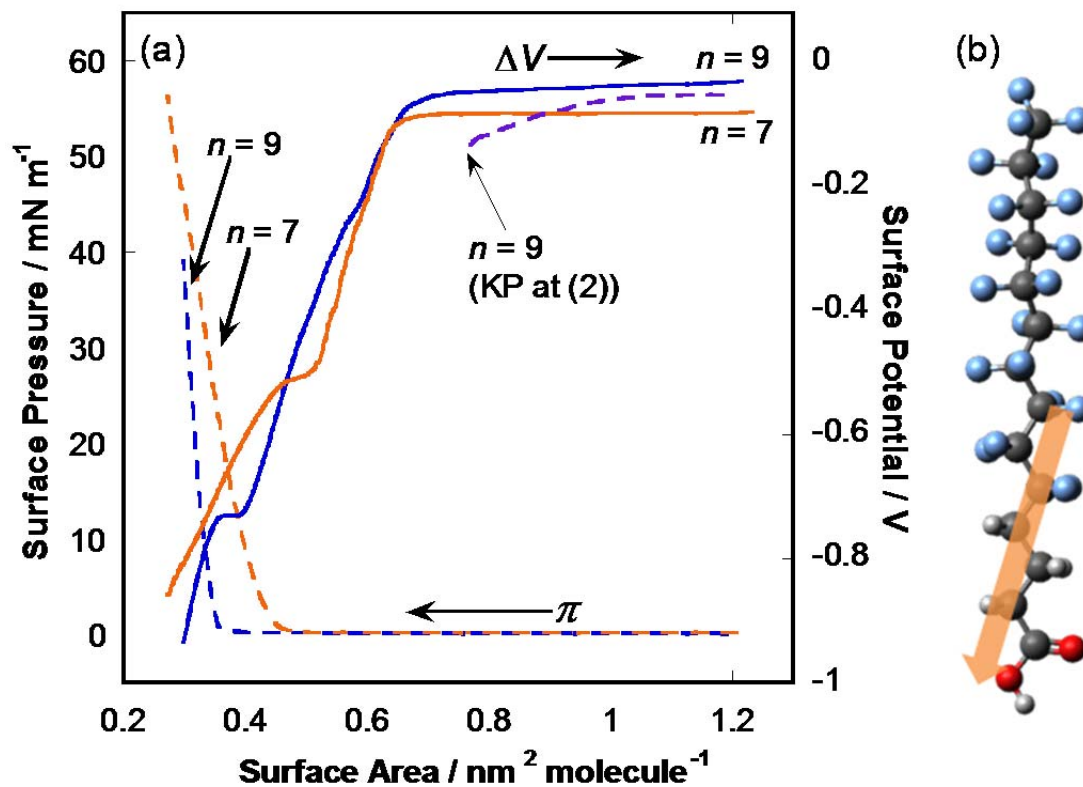
2 At the near end of the LE/LC region,  $\Delta V$  rapidly increases again. In the LC  
3 regions, the trends of the  $\Delta V$ - $A$  and  $\pi$ - $A$  isotherms are almost the same as those of SA.  
4 Therefore, the rapid increase is again attributed to the dehydration of the carboxylic  
5 group. As a conclusion, the dehydration of MA is suggested to occur twice stepwisely  
6 during the compression.

#### 7 **Analysis of MA-Rf*n* monolayers via Surface Potential Isotherms at 15 °C (Phase**

8 **II):** The  $\pi$ - $A$  isotherms of MA-Rf7 and MA-Rf9 (Figure 2a) in the present study are  
9 identical to those in the previous papers, including partially fluorinated alkanes,  
10 alcohols,<sup>4, 25-29</sup> in which no gas and LE region appear in the curves followed by a steep  
11 increase of  $\pi$ . This apparently implies that the MA-Rf7 and MA-Rf9 commonly have a  
12 spontaneous aggregation character.<sup>4</sup> To discuss the  $\Delta V$ - $A$  isotherms of MA-Rf*n* (Figure  
13 2a and 3), the molecular dipole moment of the compounds should be noted. Whereas the  
14 molecular dipole moment of SA and MA is nearly localized at the C=O group, MA-Rf*n*  
15 has a large dipole moment *along the Rf-R bond* represented as the large arrow in Figure  
16 2b and the contribution of C=O is minor as a whole.<sup>1</sup> Since the molecules of MA-Rf7  
17 and MA-Rf9 in a monolayer at 15 °C (Phase II) are oriented perpendicular to the water  
18 surface,<sup>4,28</sup> the dipole moment with a 'downward' direction should have a large

1 surface-normal component to yield a large ‘negative’  $\Delta V$ .

2



3

4 Figure 2. (a) The  $\pi$ - $A$  (dashed line) and  $\Delta V$ - $A$  (solid line) isotherms of Langmuir  
5 monolayers of MA-Rf7 (orange) and MA-Rf9 (blue) at 15 °C (phase II).  
6 The  $\Delta V$ - $A$  isotherm of MA-Rf9 displayed in purple is measured with the  
7 KP at the position of (2) in Chart 1. (b) A molecular schematic of MA-Rf9.  
8 The orange arrow represents the molecular dipole moment. The blue atoms  
9 are fluorines.

10

11 In fact, as the monolayer is compressed,  $\Delta V$  changes to a very large negative  
12 value (Figure 2a), which is specific to a diblock (Rf-R) compound.<sup>27,30</sup>  $\Delta V$  is constant at  
13 nearly zero at a surface area larger than ca.  $0.70 \text{ nm}^2 \text{ molecule}^{-1}$ . In the case of SA and

1 MA, the constant potential at nearly zero was attributed to the hydration of the  
2 carboxylic group. As for MA–Rf9, a more primitive phenomenon readily explains it,  
3 that is, the inhomogeneous distribution of the island domains. According to the SDA  
4 theory, the MA–Rf9 molecules aggregate spontaneously, and a *stiff* island domain are  
5 generated.<sup>4</sup> When a monolayer of MA–Rf9 is compressed by the moving barrier, the  
6 stiff domains should be accumulated near the barrier; whereas the domains near the  
7 Kelvin probe at the position (1) in Chart 1 would be left un-compressed at the initial  
8 stage.

9 To confirm this speculation, the same measurements were carried out by  
10 displacing the Kelvin probe to the position (2) in Chart 1. As expected,  $\Delta V$  decreases  
11 earlier (the purple dashed line in Figure 2a), which proves that the stiff domains near the  
12 barriers are collected to arrive at the position (2) earlier. The inhomogeneity model has  
13 thus been confirmed readily. MA–Rf7 (orange curve) exhibits a similar process, but the  
14 initial constant potential is a little shifted to a negative value, which will be discussed in  
15 detail in the next section.

16 During the decrease of  $\Delta V$ , an “apparent plateau” appears just before the lift-off  
17 of  $\pi$  for both MA–Rf7 ( $A \approx 0.5$ ) and MA–Rf9 ( $A \approx 0.4$ ). The relative position of the  
18 change of  $\pi$  and  $\Delta V$  straightforwardly implies that the cancel of the decreasing potential

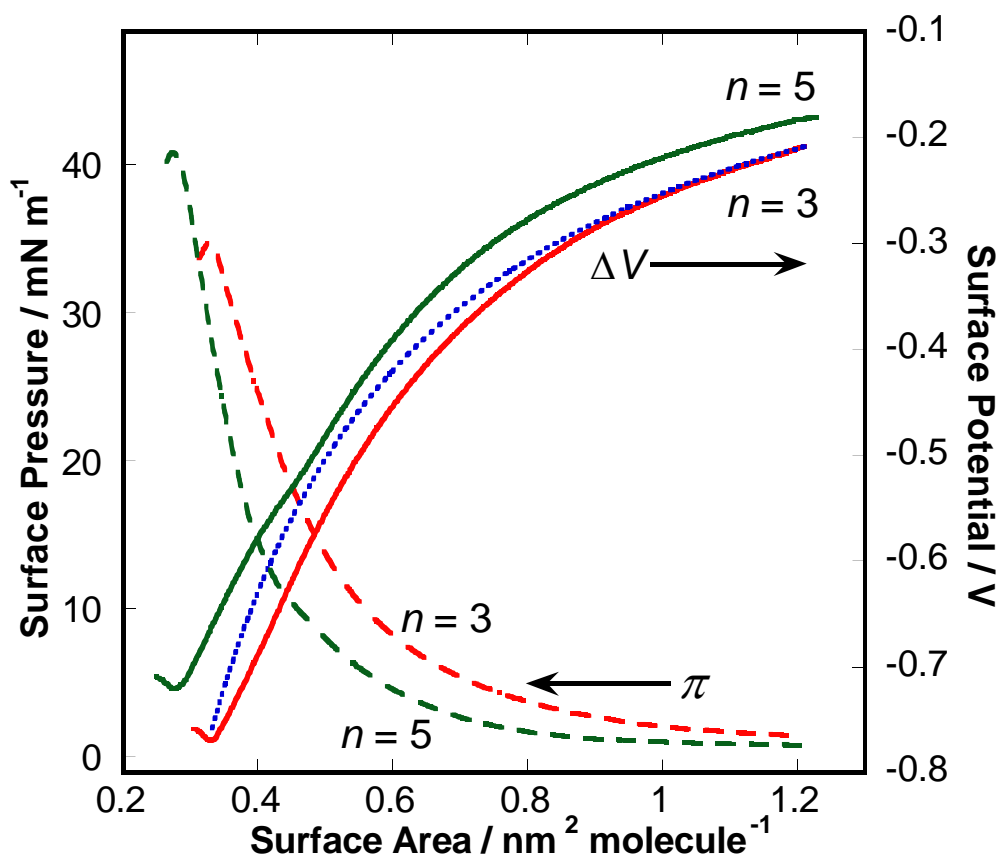
1 should be attributed to the dehydration of the carboxylic group, since the dehydration  
2 generates the positive increase of the potential.

3 In the case of SA and MA, the potential increase due to the dehydration cannot  
4 be discriminated from the increasing density, since both changes exhibits positive  
5 changes. On the other hand, in the case of an Rf-R diblock compound, the two changes  
6 exhibit opposite potential changes, which make the dehydration process clearly visible.

7 On the other hand, the molecules of MA-Rf3 and MA-Rf5 having a shorter Rf  
8 chain have a poor aggregation property, which is quite different from MA-Rf7 and  
9 MA-Rf9.<sup>4</sup> As found in the isotherms in Figure 3,  $\pi$  exhibits an apparent positive value  
10 even at an initial compression, which indicates that molecules are lying on the water  
11 surface.<sup>4</sup> As discussed for normal MA shown in Figure 1b, the spread molecules do not  
12 make island domains, but they are spread over the water surface homogeneously.

13 The  $\Delta V$ - $A$  isotherms of the MA-Rf3 and MA-Rf5 monolayers are overlaid on  
14 the  $\pi$ - $A$  isotherms in Figure 3. The  $\Delta V$  curves of MA-Rf3 and MA-Rf5 decrease  
15 significantly as compressed, which agrees with the density curve (blue dotted curve; ( $A_0$ ,  
16  $\Delta V_0$ ) = (1.211, -0.208)). This agreement confirms that the molecules are, in fact,  
17 homogeneously spread over the water surface for both compounds.

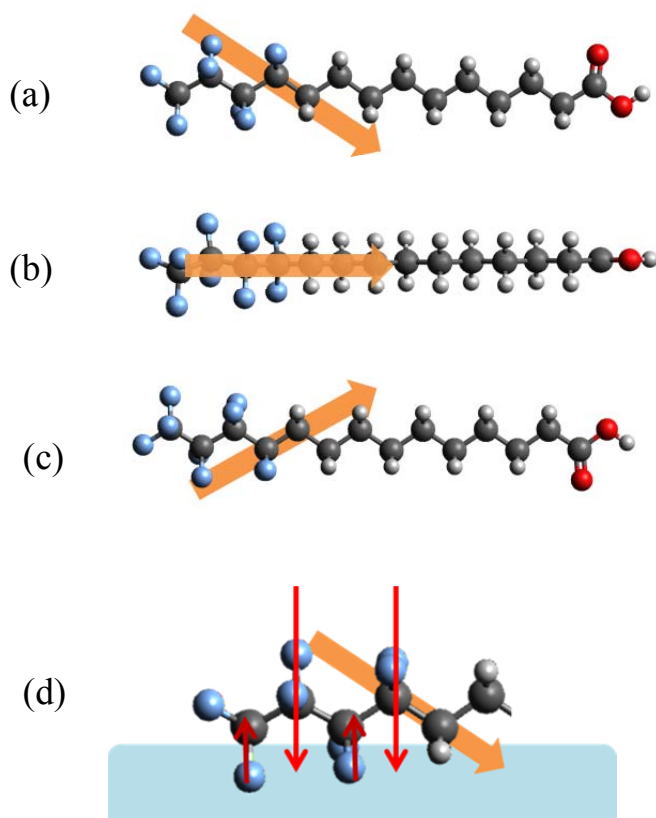
18



1  
 2 Figure 3. The  $\pi$ - $A$  (dashed line) and  $\Delta V$ - $A$  (solid line) isotherms of Langmuir  
 3 monolayers of MA-Rf3 (red) and MA-Rf5 (green) at 15 °C (phase II). The  
 4 blue dotted line is a calculated density curve.

5  
 6 Here, we have to pay attention to a fact that  $\Delta V$  exhibits a fairly large negative  
 7 value “even before” the monolayer compression, which is apparently larger than that in  
 8 Figure 2a. If the molecules are lying on the water surface, there is no need to exhibit a  
 9 negative value considering various molecular rotational orientations of the lying  
 10 molecule (Figure 4a–c). Water surface is known to have hydrogen-bond free (dangling)  
 11 OH groups,<sup>12</sup> which can receive a single Rf group via the dipole-dipole interaction. In

1 this manner, a single Rf group lying on the water surface would be highly stabilized via  
2 the dipole-interactive property. In addition, a single Rf group is not dissolved into a  
3 bulky water, since the Rf group has only the dipole-interactive character, and no  
4 hydrogen bonding one, which is unfavorable to break the hydrogen bonding network of  
5 the bulky water. As a result, a single Rf group is stably interacted with water ‘surface’  
6 only.



26 Figure 4. (a)~(c) Three different rotational orientations of a lying MA-Rf3 molecule.  
27 (d) A schematic view of a dipole-interactive Rf group in the water surface  
28 based on the schematic (a).

1           The lying molecular scheme (Figure 4d) works well for explaining the potential  
2 isotherms. In this model, one side of the lying Rf group is attached to the water surface,  
3 and the rest half remains un-hydrated. This partial hydration model implies that each  
4 dipole moment on the hydrated side is shielded, and the negative potential should  
5 appear as a total irrespective of the rotational molecular orientation on the water surface.

6

7   **Prediction of Phase Transition by the SDA theory:** The analytical discussion made  
8 above is for a fixed temperature of 15 °C, i.e., Phase II. In the present section, the bulk  
9 material properties of monolayers in Phase IV<sup>12</sup> are predicted on the SDA theory.

10           The SDA theory provides a criterion<sup>4</sup> whether the spontaneous two-dimensional  
11 molecular aggregation of Rf groups takes place or not, which depends on the twisting  
12 angle of the Rf group reflecting the Rf length (Table 1). When the theoretical twisting  
13 angle is 90° or larger, they are expected to aggregate spontaneously.<sup>4</sup> When referring to  
14 Table 1, below 19 °C, MA-Rf $n$  is spontaneously aggregated for  $n = 7$  and 9 (marked by  
15 bold in Table 1); whereas only MA-Rf9 should be aggregated above 19 °C. This implies  
16 that only MA-Rf7 would exhibit an apparent change in both  $\pi$ -A and  $\Delta V$ -A isotherms  
17 when the measurement temperature is changed from 15 °C to 25 °C.

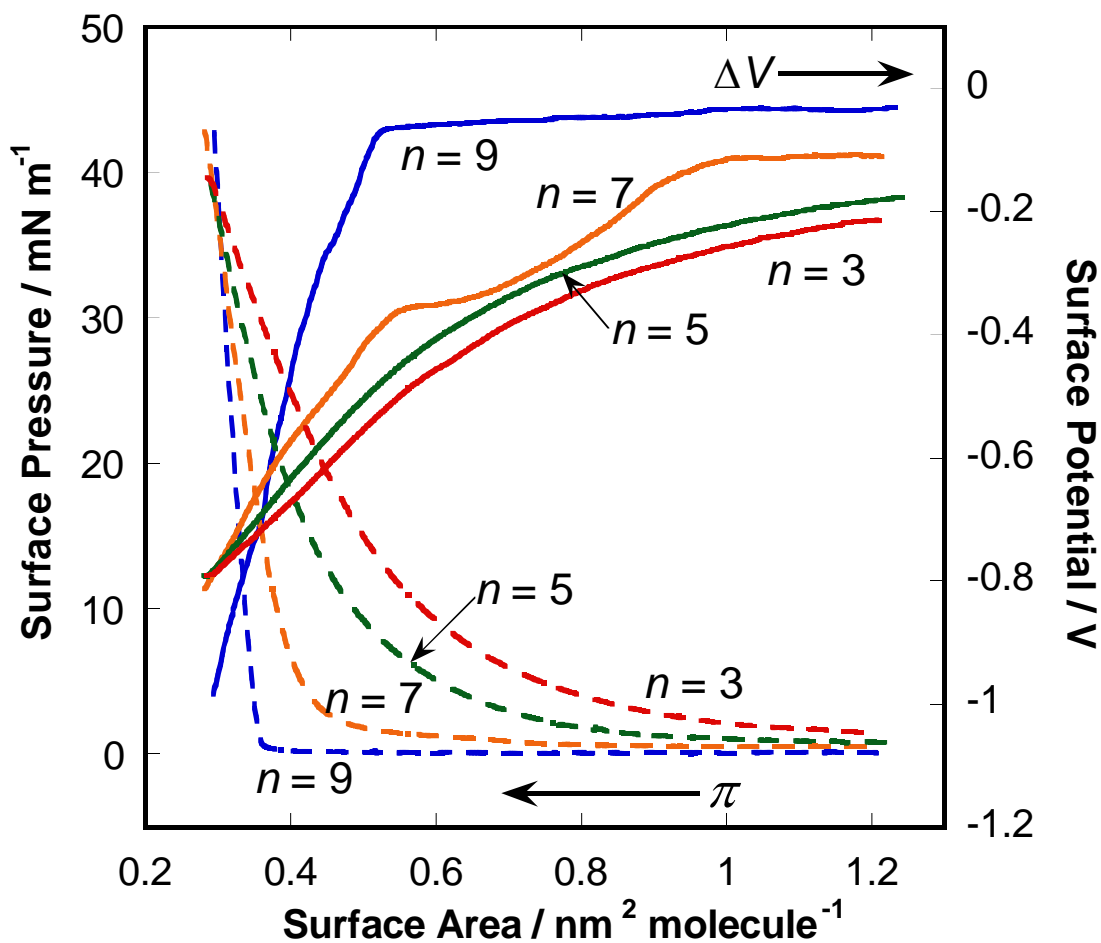
18

**Table 1 Theoretical twisting angle of both ends of the CF<sub>2</sub> groups in an Rf group as a function of the number of CF<sub>2</sub> groups (Rf length) in Phases II and IV.**

No. of CF <sub>2</sub>	Twisting angle / °	
	Phase II (<19 °C)	Phase IV (>19 °C)
3	Un-twisted	Un-twisted
5	60	51
7	<b>90</b>	77
9	<b>120</b>	<b>103</b>

Figure 5 presents the  $\pi$ - $A$  and  $\Delta V$ - $A$  isotherms of MA-Rf $n$  monolayers on water at 25 °C.  $\Delta V$ - $A$  isotherms (solid lines) are particularly sensitive to the Rf length and temperature. As theoretically predicted on the SDA theory, only the  $\Delta V$ - $A$  isotherm of MA-Rf7 (orange curve) is significantly changed from that in Figure 2a; whereas the rest curves are kept almost unchanged. The potential decrease below the surface area of 0.9 nm<sup>2</sup> molecule<sup>-1</sup> in Figure 5 is more apparent than that of Figure 2a. The early decrease implies that the molecules at 25 °C are more homogeneously spread on water than 15 °C. The decrease is suppressed at 0.7 nm<sup>2</sup> molecule<sup>-1</sup> or smaller, which indicates that dehydration happens in this region because  $\pi$  begins to increase after the suppress finishes in an exchanging fashion. In this manner, only the MA-Rf7 monolayer exhibits different aggregate properties in both  $\pi$ - $A$  and  $\Delta V$ - $A$  isotherms as predicted by the SDA theory.





1  
2  
3 Figure 5. The  $\pi$ -A (dashed line) and  $\Delta V$ -A (solid line) isotherms of Langmuir  
4 monolayers of MA-Rf3 (red), MA-Rf5 (green), MA-Rf7 (orange) and  
5 MA-Rf9 (blue) at 25 °C (phase IV).

6  
7 Reproducibility of  $\Delta V$ -A isotherm measurements is another useful index to

8 check the homogeneity of the monolayer. When a monolayer of homogeneously spread

9 molecules is compressed, the  $\Delta V$ -A measurements shows a good reproducibility;

10 whereas a monolayer of island domains shows a poor reproducibility.<sup>31</sup> Figure 6 shows

1 three traces for each  $\pi$ -A and  $\Delta V$ -A isotherm of MA-Rf3 and MA-Rf7. As shown in  
2 Figure 6a, MA-Rf3 at 15 °C shows an extremely high reproducibility, and the same  
3 trend is also found at 25 °C (data not shown), which is consistent with a fact that a short  
4 Rf compound does not show an apparent aggregation.<sup>4</sup> On the other hand, MA-Rf7  
5 shows a good reproducibility at 25 °C; whereas the reproducibility is lost at 15 °C in the  
6 area range of 0.4~0.6 nm<sup>2</sup> molecule<sup>-1</sup>, which straightforwardly implies that the  
7 molecules are aggregated to generate island domains at 15 °C, while they are spread  
8 homogeneously at 25 °C. The results are perfectly consistent with the theoretical  
9 prediction on the SDA theory (Table 1).

10

11

12

13

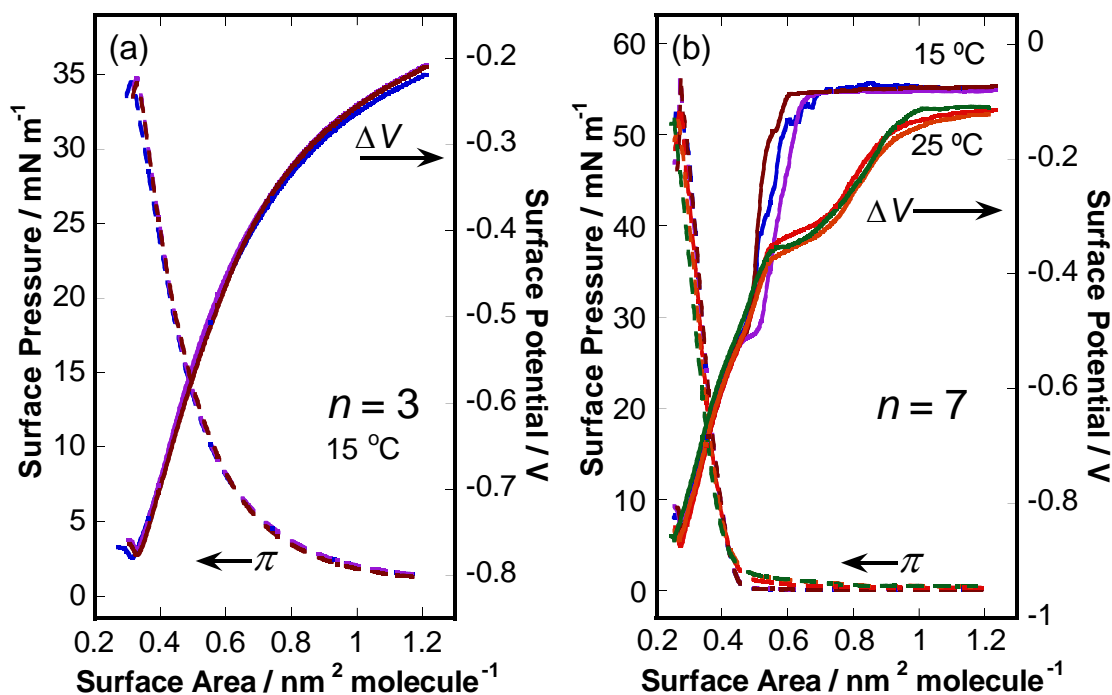


Figure 6. The  $\pi$ -A (dashed lines) and  $\Delta V$ -A (solid lines) isotherms of the monolayers of (a) MA-Rf3 and (b) MA-Rf7. Three repeatedly measured results are overlaid for checking the reproducibility. Only the results at 15 °C are presented for better visibility in (a), since no difference was found for both 15 °C and 25 °C.

The reader may be interested in the results of MA-Rf9 at 25 °C, since the suppression of the potential decrease during the monolayer compression is not obvious (Figure 5) when comparing to the results at 15 °C. On closer inspection, however, the suppression gradually appears along the potential decrease. Since the reproducibility of this isotherm was high, the hydrated water should smoothly and gradually be removed at 25 °C on the compression probably due to a high molecular mobility at a higher temperature.

1 **Conclusion:** Through the comparative study of the surface potential ( $\Delta V$ )–surface area  
2 (A) isotherm of a monolayer of a carboxylic acid involving a normal alkyl and a  
3 perfluoro alkyl (Rf) group with a different length, the dehydration process is found to be  
4 a key to understand the isotherms, which is a progress to the conventional discussion on  
5 only the molecular density and orientation changes [15]. The ‘dehydration’ effect would  
6 be useful for understanding the properties of a Langmuir monolayer of a wide range of  
7 compounds, not only for Rf compounds. In particular for an Rf containing diblock  
8 compound, the dehydration process is apparently visible in the isotherm, which greatly  
9 helps us to discuss the surface pressure ( $\pi$ )–A isotherm, too. As a result, the  $\Delta V$   
10 measurements have proved to be powerful to discriminate whether the compound has a  
11 spontaneous molecular aggregation property or not. In addition, a lying Rf-R diblock  
12 molecule has been revealed to have a “dipole-interactive property” on the Rf group. A  
13 “single” Rf group is interacted with the water surface, but it is not dissolved in the bulky  
14 water. In other words, the water surface has proved to have a unique chemical field to be  
15 interacted with an Rf group. Regardless, a further molecular orientation study is  
16 expected to fully confirm the discussion in this study. To do that, we are planning an  
17 additional study using the polarization modulation-infrared reflection- absorption  
18 spectrometry (PM-IRRAS) technique, which can measure IR spectra of a Langmuir

1 monolayer on the water surface in situ [23,24].

2

## 1   **ACKNOWLEDGMENT**

2       This work was financially supported by Grant-in-Aid for Young Scientists (B) [No.  
3   26810075(TS)] and Grant-in-Aid for Scientific Research (A) (No. 15H02185 (TH))  
4   from Japan Society for the Promotion of Science, the Collaborative Research Program  
5   of Institute for Chemical Research, Kyoto University (grant no. 2015-87 (MS)), and the  
6   “Element Innovation” Project by the Ministry of Education, Culture, Science, Sports  
7   and Technology of Japan (MEXT), for which the authors thanks are due.

## 8   **REFERENCES:**

- 9   1.   Krafft, M. P.; Riess, J. G. *Chemistry, Physical Chemistry, and Uses of Molecular*  
10       *Fluorocarbon–Hydrocarbon Diblocks, Triblocks, and Related Compounds—Unique*  
11       *“Apolar” Components for Self-Assembled Colloid and Interface Engineering.*  
12       *Chem. Rev.* **2009**, *109*, 1714–1792.
- 13   2.   Minkin, V. I.; Osipov, O. A.; Zhdanov, Y. A. *Dipole Moments in Organic*  
14       *Chemistry*; Plenum Press: New York, 1970.
- 15   3.   Huheey, J. E. *Inorganic Chemistry*; Harper&Row: New York, 1978.
- 16   4.   Hasegawa, T.; Shimoaka, T.; Shioya, N.; Morita, K.; Sonoyama, M.; Takagi, T.;  
17       Kanamori, T. Stratified Dipole-Arrays Model Accounting for Bulk Properties

- 1 Specific to Perfluoroalkyl Compounds. *ChemPlusChem* **2014**, 79, 1421–1425.
- 2 5. London, F. The General Theory of Molecular Forces. *Trans. Faraday Soc.* **1937**, 8–  
3 26.
- 4 6. Bunn, C. W.; Howells, E. R. Structures of Molecules and Crystals of Fluorocarbons.  
5 *Nature* **1954**, 174.
- 6 7. Ute, K.; Kinoshita, R.; Matsui, K.; Miyatake, N.; Hatada, K. Conformational  
7 Asymmetry of a Linear Perfluoroalkyl Chain in Solution. Dynamic Fluorine-19  
8 NMR Spectroscopy of the Perfluoro-*n*-Alkanes Carrying a Chiral End-Group as a  
9 Probe of Magnetic Nonequivalence. *Chemistry Letters* **1992**, 1337–1340.
- 10 8. Thomas, R. R. Material properties of fluoropolymers and perfluoroalkyl-based  
11 polymers (Chapter 2), *Fluoropolymers, vol. 2*, Springer: Heidelberg, 1999.
- 12 9. Hasegawa, T. Understanding of the Intrinsic Difference between Normal- and  
13 Perfluoro-Alkyl Compounds toward Total Understanding of Material Properties.  
14 *Chem. Phys. Lett.* **2015**, 627, 64–66.
- 15 10. Skrabania, K.; von Berlepsch, H.; Böttcher, C.; Laschewsky, Synthesis of Ternary,  
16 Hydrophilic-Lipophilic-Fluorophilic Block Copolymers by Consecutive RAFT  
17 Polymerizations and Their Self-Assembly into Multicompartment Micelles A.  
18 *Macromol.* **2010**, 43, 271–281.

- 1 11. Wakai, C.; Shimoaka, T.; Hasegawa, T. Characterization of Adsorbed Molecular  
2 Water on the Surface of a Stretched Polytetrafluoroethylene Tape Analyzed by <sup>1</sup>H  
3 NMR. *J. Phys. Chem. B* **2016**, *120*, 2538–2543.
- 4 12. Goto, T.; Ikehata, A.; Morisawa, Y.; Ozaki, Y. Surface Effect of Alumina on the  
5 First Electronic Transition of Liquid Water Studied by Far-Ultraviolet Spectroscopy.  
6 *J. Phys. Chem. Lett.* **2015**, *6*, 1022–1026.
- 7 13. Ariga, K.; Yamauchi Y.; Mori, T.; Hill J. P. 25th Anniversary Article: What Can Be  
8 Done with the Langmuir-Blodgett Method? Recent Developments and its Critical  
9 Role in Materials Science, *Adv. Mater.* **2013**, *25*, 6477-6512.
- 10 14. Albrecht, O.; Matsuda, H.; Eguchi, K.; Nakagiri, T. The Dissolution of Myristic  
11 Acid Monolayers in Water. *Thin Solid Films* **1999**, *338*, 252–264.
- 12 15. Gains, G. L., Jr. *Insoluble monolayers at liquid-gas interface*; John Wiley & Sons,  
13 Inc: New York, 1966.
- 14 16. Clark, E. S. The Molecular Conformations of Polytetrafluoroethylene: Forms II and  
15 IV. *Polymer* **1999**, *40*, 4659–4665.
- 16 17. Yamins, H. G.; Zisman, W. A New Method of Studying the Electrical Properties of  
17 Monomolecular Films on Liquids. *J. Chem. Phys.* **1933**, *1*, 656.
- 18 18. Kang, Y. S.; Lee, D. K.; Kim, Y. S. A Study on Temperature Dependency and in



- 1 Situ Observation of Domain Structure in Langmuir Layers of Stearic Acid/ $\gamma$ -Fe<sub>2</sub>O<sub>3</sub>  
2 Nanoparticle Complex at the Air/water Interface. *Synthetic Metals* **2001**, *117*, 165–  
3 167.
- 4 19. MacRitchie, F. Monolayers (Chapter 7), *Chemistry at Interfaces*, Academic Press:  
5 San Diego, **1990**.
- 6 20. Kaganer, V. M.; Möhwald, H.; Dutta, P. Structure and Phase Transitions in  
7 Langmuir Monolayers. *Rev. Mod. Phys.* **1999**, *71*, 3, 779–819.
- 8 21. Ouyang, B.; Howard, B. J. High-Resolution Microwave Spectroscopic and Ab  
9 Initio Studies of Propanoic Acid and Its Hydrates. *J. Phys. Chem. A* **2008**, *112*,  
10 8208–8214.
- 11 22. Tanaka, H.; Hayashi, K.; Akatsuka, T.; Toyama, J.; Noda, K.; Kida, T.; Ogoma, Y.;  
12 Fujii, T.; Kondo, Y. Morphology of a Cytochrome *c*-Adsorbed Stearic Acid  
13 Monolayer on Brewster Angle Microscopy. *J. Biochem.* **1995**, *117*, 1151–1155.
- 14 23. Muro, M.; Itoh, Y.; Hasegawa, T. A Conformation and Orientation Model of the  
15 Carboxylic Group of Fatty Acids Dependent on Chain Length in a Langmuir  
16 Monolayer Film Studied by Polarization-Modulation Infrared Reflection  
17 Absorption Spectroscopy. *J. Phys. Chem. B* **2010**, *114*, 11496–11501.
- 18 24. Calvez, E.; Blaudez, D.; Buffeteau, T.; Desbat, B. Effect of Cations on the

- 1       Dissociation of Arachidic Acid Monolayers on Water Studied by  
2       Polarization-Modulated Infrared Reflection–Absorption Spectroscopy. *Langmuir*  
3       **2001**, *17*, 670–674.
- 4   25. Maaloum, M.; Muller, P.; Krafft, M. P. Monodisperse Surface Micelles of Nonpolar  
5       Amphiphiles in Langmuir Monolayers. *Angew. Chem.* **2002**, *41*, 4331–4334.
- 6   26. Lux, C.; Gallani, J.; Waton, G.; Krafft, M. P. Compression of Self Assembled Nano  
7       Objects: 2D/3D Transitions in Films of (Perfluoroalkyl) Alkanes Persistence of an  
8       Organized Array of Surface Micelles. *Chem. - Eur. J.* **2010**, *16*, 7186–7198.
- 9   27. Broniatowski, M.; Dynarowicz-Łątka, P. Semifluorinated Alcohols in Langmuir  
10      monolayers—A Comparative Study. *J. Colloid Interface Sci.* **2006**, *301*, 315–322.
- 11   28. Hasegawa, T.; Shimoaka, T.; Tanaka, Y.; Shioya, N.; Morita, K.; Sonoyama, M.;  
12      Amii, H.; Takagi, T.; Kanamori, T. An Origin of Complicated Infrared Spectra of  
13      Perfluoroalkyl Compounds Involving a Normal Alkyl Group. *Chem. Lett.* **2015**, *44*,  
14      834–836.
- 15   29. Kato, T; Kameyama, M; Ehara, M; Iimura, K. Monodisperse Two-Dimensional  
16      Nanometer Size Clusters of Partially Fluorinated Long-Chain  
17      Acids. *Langmuir* **1998**, *14*, 1786–1798.
- 18   30. Bennett, M. K.; Zisman, W. A. The Behavior of Monolayers of Progressively

- 1 Fluorinated Fatty Acids Adsorbed on Water. *J. Phys. Chem.* **1963**, *67*, 1534–1540.
- 2 31. Harkins, W. D.; Fischer, E. K. Contact Potentials and the Effects of Unimolecular
- 3 Films on Surface Potentials. I. Films of Acids and Alcohols. *J. Chem. Phys.* **1933**, *1*,
- 4 852–862.